

7 Comparison of Analytical and Finite-Element Models

7.1 INTRODUCTION

The finite element model was developed as an alternative to the simpler analytical model. Comparisons were made to verify both models would produce similar results under similar testing variables. This chapter explains the comparisons made and details the pros and cons of each model.

7.2 APPLIED STRESS INTENSITY FACTOR COMPARISONS

The basis for both the analytical and F.E. model is the ability to predict the applied stress intensity factor. The applied stress intensity factor is the same whether gap elements are used or not in a F.E. analysis. Figure 7-1 demonstrates the applied stress intensity factor for both maximum and minimum stress in the specimen with solid stiffeners, case 1.

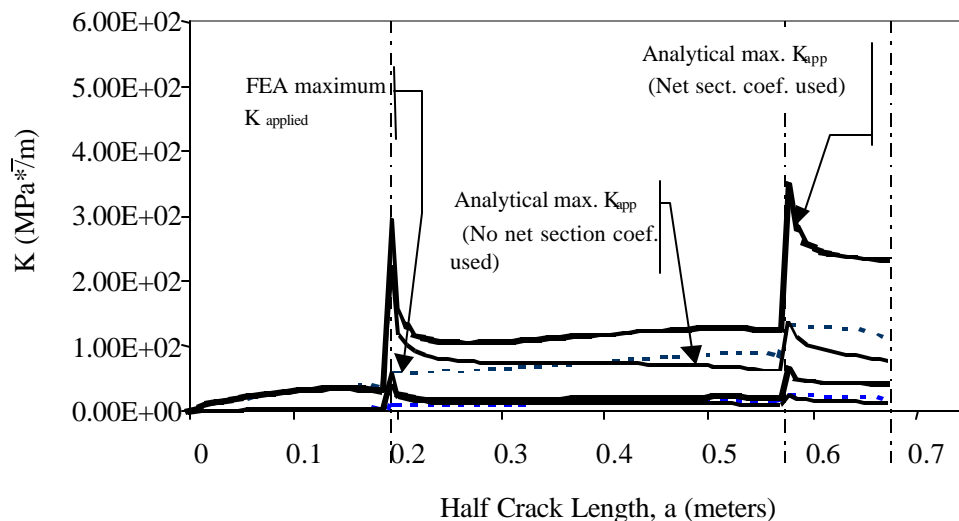


Figure 7-1: $K_{app,max}$ and $K_{app,min}$ for both finite element and analytical models, immediately severed stiffeners.

This plot depicts the assumption that the stiffeners are severed immediately once the crack has reached them. Only the maximum K_{app} curves have been pointed out to prevent clutter in the figure, but the type of line is held constant in the minimum K_{app} curves. Better agreement between the analytical and finite element models is obtained if the net section coefficient is not used in the analytical model. This characteristic will be noted in many of the comparisons.

Interpolation between intact and severed stiffeners is seen in Figure 7-2. Here the results shown in Figure 7-1 have merely included the assumption of equal growth rates in the stiffener and the plate.

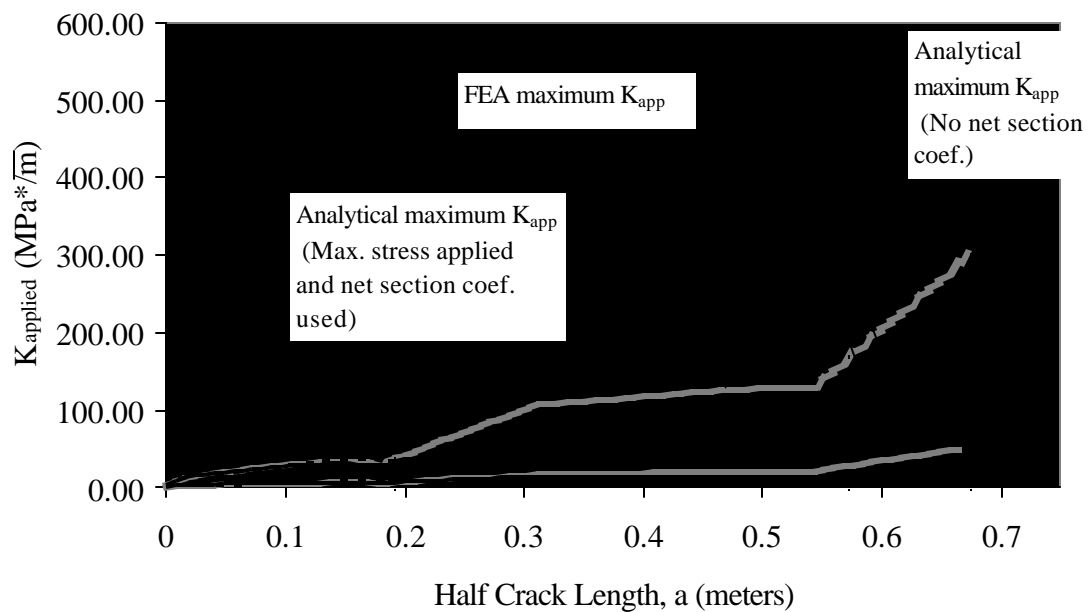


Figure 7-2: $K_{app,max}$ and $K_{app,min}$ for both finite element and analytical models, stiffener interpolation used.

These comparisons show that good duplication between the analytical and finite element models exist without residual stresses included.

7.3 RESIDUAL STRESS INTENSITY FACTOR COMPARISON

The next comparison made was that of the residual stress intensity factor. The residual stress intensity factor showed the most scatter between models. Varied results were attained between the models, and therefore a more in-depth study was made concerning the overall effects on K_{total} . Figure 7-3 shows the different curves that comprised the study.

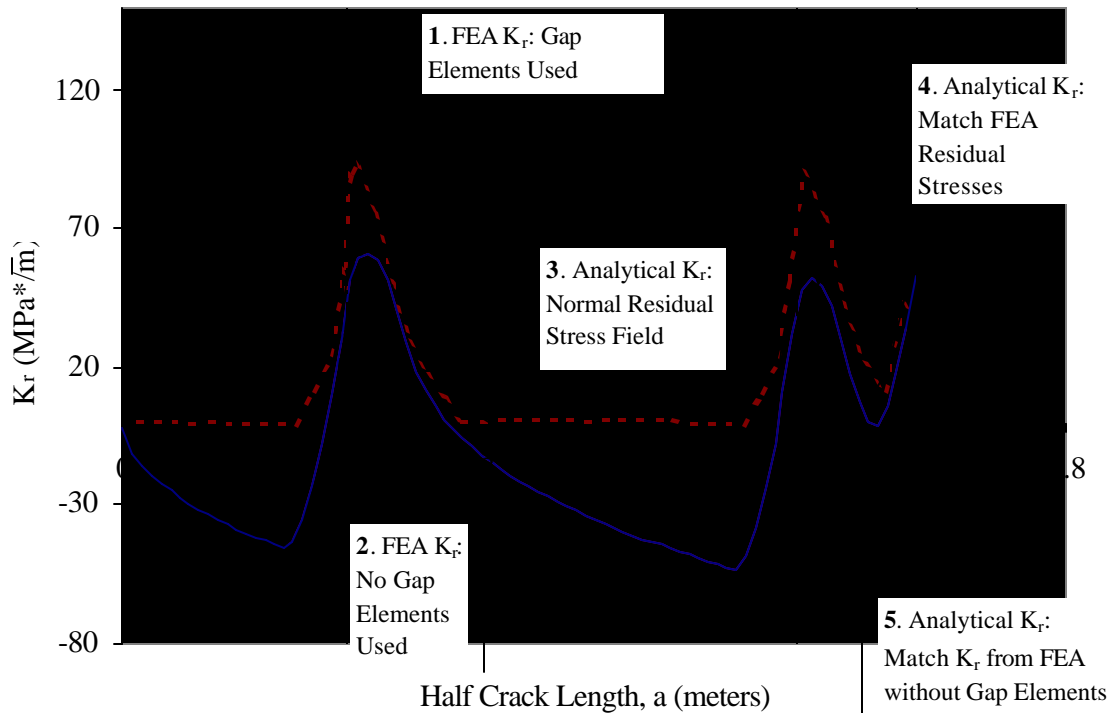


Figure 7-3: K_r for both finite element and analytical models.

The study included the following components:

1. The finite element K_r obtained using gap elements and upper bound residual stress.
2. The finite element K_r obtained without gap elements (Extrapolated from the gap element analysis with upper bound residual stress).
3. K_r from an analytical model using a typical Faulkner residual stress determination.
4. K_r from analytical model using the same residual stress distribution input into the finite element models (F.E. upper bound residual stress)

5. K_r from an analytical model that matches K_r from number 2. Iteration was used to determine the residual stress distribution necessary in the analytical model to reproduce the K_r derived in study point two.

Figure 7-3 has several characteristics that may be immediately observed. First, K_r from curve 1 never becomes negative. This is because the gap elements were specified with an initial gap of zero meters. Consequently, J remains zero in compressive residual stress regions until sufficient external load is applied to separate the crack faces.

In the F.E. analysis without gap elements, curve 2, J values and subsequent K_r values were determined by subtracting K_{app} from K_{total} . Recall the criteria that, in order to perform this extrapolation, the external load must at least match the opening load before K_r can be obtained. It is not clear why this K_r differs significantly from K_r in curve 1), and so both K_r values were studied in their correlation with the analytical model.

Analytical modeling provided residual stress intensity factors that corresponded well within the range suggested by both F.E. analyses. When the residual stress distribution that was created in the finite element analysis was used in the analytical model, a K_r resulted (Curve 4) that averaged both finite element analyses. Increasing the residual compressive stresses in the analytical model allowed curve 5 to be formulated. Finally, curve 3 shows that K_r obtained by using Faulkner's residual stress distribution provides an average K_r curve that emulates the gap element K_r quite well. The Faulkner residual stress distribution is what would normally be used in a standalone analytical model, where residual stress values are not obtained in connection with F.E. modeling. The excellent correlation with the finite element K_r curves promotes its use as a simplification to the more complex F.E. modeling.

7.4 TOTAL STRESS INTENSITY FACTOR COMPARISONS

Minute differences in K_r and K_{app} between the models have been very acceptable in the results presented so far. The additive effects of these differences are seen in comparing K_{total} for the various analyses. Figure 7-4 plots each K_{total} curve for direct comparison.

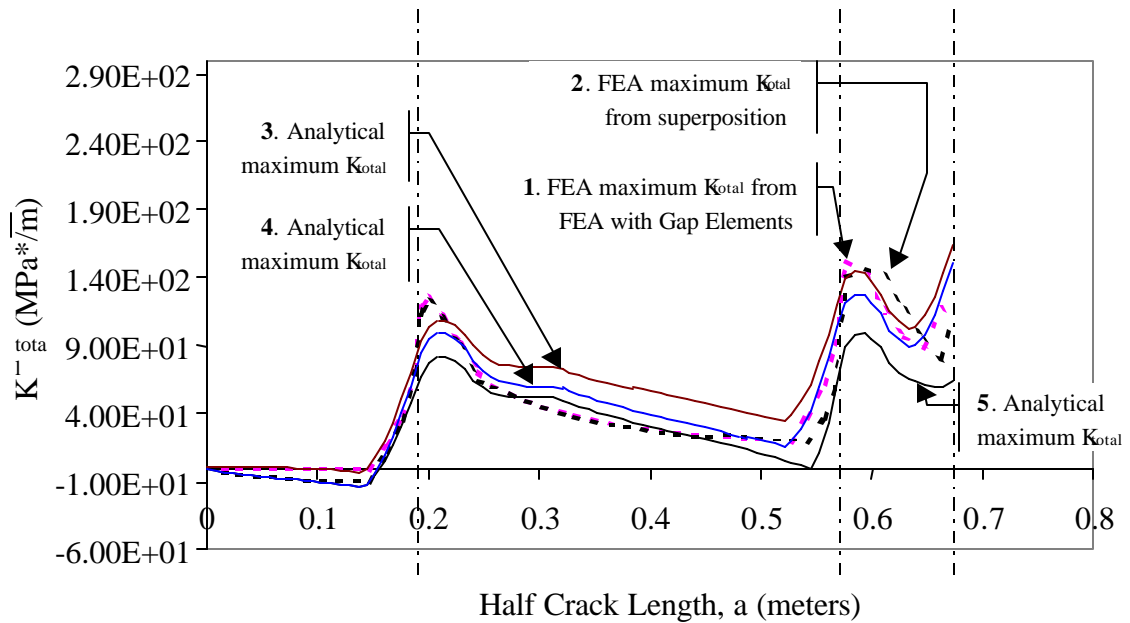


Figure 7-4: K_{total} for both finite element and analytical models.
(Analytical results do not include a finite width correction.)

No finite width correction was used in the analytical curves. Good agreement seems consistent throughout the models plotted in Figure 7-4. However, small variations in K_{total} are cubed in the Paris Law, so it is important to correctly identify which curve is most appropriate. For example, curve 5 would predict cracking stop altogether at 545-mm while the other models do not indicate this drastic a reduction in K_{total} .

Degraded correlation is seen when the net section coefficient or other finite width correction is used in the analytical model. Figure 7-5 shows the increased K_{total} values in the analytical model.

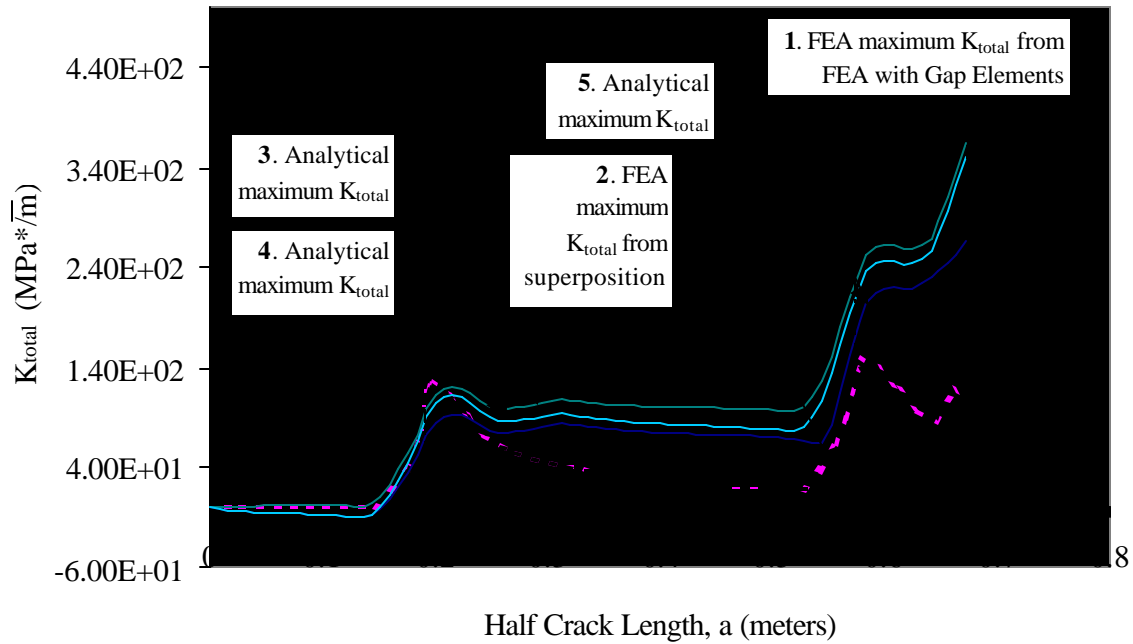


Figure 7-5: K_{total} for both finite element and analytical models.
(Finite width correction included in analytical models.)

7.5 STRESS INTENSITY FACTOR RANGE COMPARISONS

Comparing ΔK provides the most direct view of discrepancies between F.E. and analytical modeling. The comparison is also the most significant because these values are cubed in the Paris Law for crack growth prediction. Two figures are put forth to demonstrate the results: Figure 7-6 plots ΔK_{app} and Figure 7-7 plots ΔK_{eff} . Once again it may be seen that the net section coefficient decreases the compliance between the models.

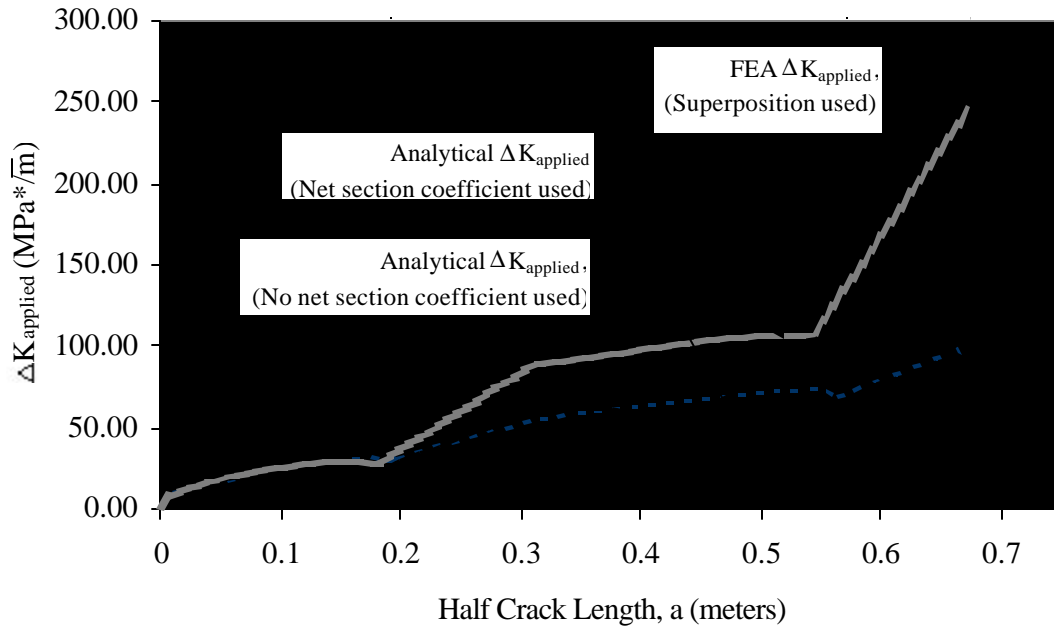


Figure 7-6: ΔK_{app} for both finite element and analytical models.
 (Analytical results do not include a finite width correction.)

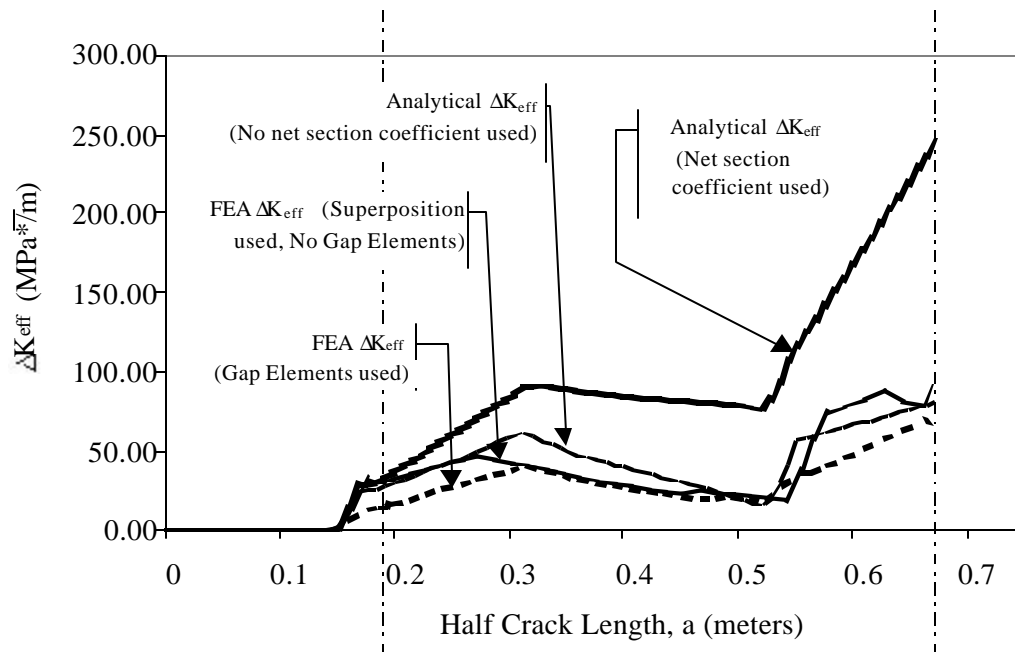


Figure 7-7: ΔK_{eff} for both finite element and analytical models.
 (Finite width correction included in analytical models.)

The increase in error caused by including the net section coefficient is difficult to explain. One reason may be that the increase in net section stress is not realized until the full panel width is cracked and a crack has entered the edge web. The edge web might be providing sufficient restraint to reduce the effects of increased net section stresses. This uncertainty should be investigated further, but the true test of the models is their ability to predict the experiments.

As will be seen in the next chapter, experimental comparisons support neglecting the finite width correction. However, the net section correction for cracks in ship hulls will likely be very close to unity for even long cracks. For this reason, it could be used to add an increased factor of safety to one's predictions.

8 Prediction Success with Experimental Cases

8.1 INTRODUCTION

Previously it has been shown that the analytical model can readily be used to obtain the same results as the finite element model. This fact was taken advantage of in refining the analysis to produce better results. For example, instead of re-running a complete set of F.E. analyses with a different residual stress field the analytical model was used with the new residual stress field input. The result was then obtained in three minutes as opposed to several days of running F.E. analyses and J value interpolation.

Many variables affected the predictions made in the stiffened panels. Correlation between the analytical and finite element model alone required a number of investigations to be made. These investigations led to observations that were necessary to develop a cohesive set of results under the same conditions. The same procedure will be taken in the following sections.

It is not enough to show the final results and expect an individual to reproduce them under the same conditions without certain error. Therefore, the focus of the predictions will be the revisions made to achieve good results. With this approach, one will learn the correct procedure while avoiding the pitfalls that had occurred in developing the current final results.

8.2 BASELINE SPECIMEN

Determining the applied stress ranges and values is the most significant source of error in prediction accuracy. Such difficulty was realized early on in baseline case predictions. The initial predictions were made using the average of the three strain gages mounted at 76-cm.

from the crack line (See Figure 3-7). These predictions, shown in Figure 8-1, indicated that the correct uniform stress should be higher and within the constant moment region of the experiment configuration. Good correlation with the experiments was obtained using a uniform stress as indicated in Figure 3-8.

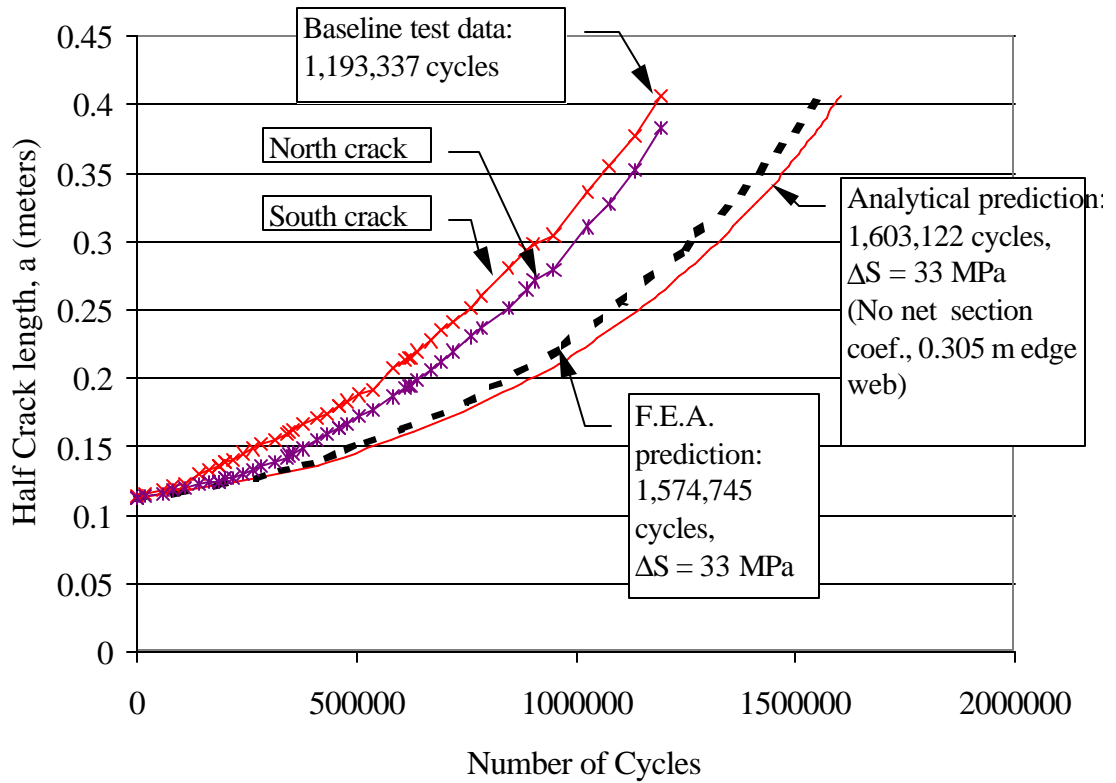


Figure 8-1: Initial predictions made for baseline test specimen.

This location of stress monitoring was used for the remainder of the experiment predictions to prevent bias in one prediction over another. The prediction based on the final stress measurement point is shown in Figure 8-2.

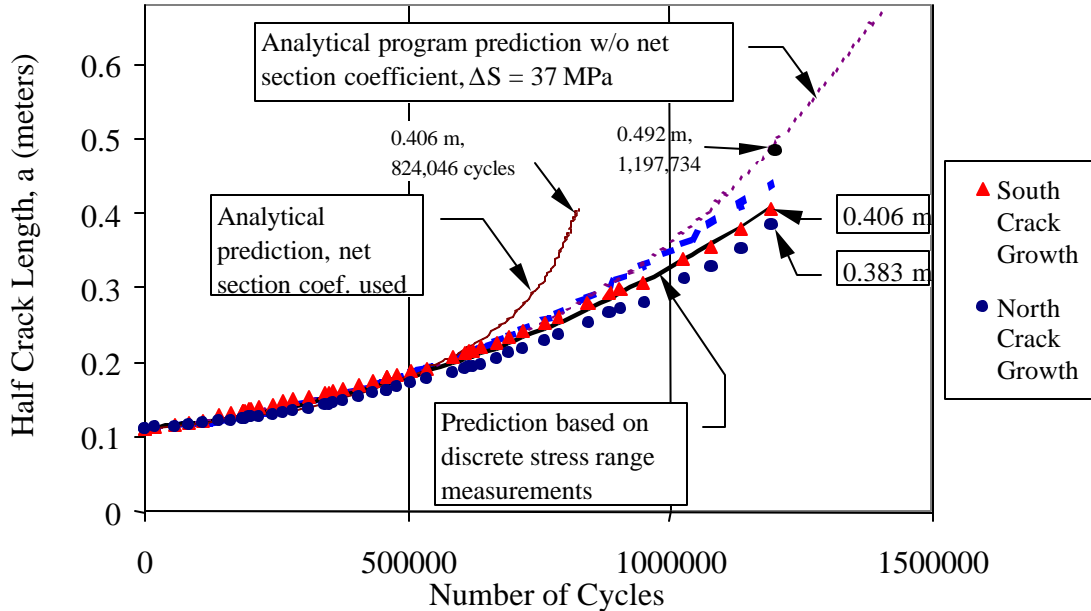


Figure 8-2: Final predictions made for baseline test specimen.

Note that use of a finite width correction dramatically skews the accuracy of the prediction (The finite width correction in these analyses is made by using the net section coefficient). The finite width correction is seen as the only contributor to the error, because the error becomes exponentially larger as the crack becomes larger. If the error were due to improper stress definition, the deviation from the experimental results would be consistent from the initial crack lengths.

The excellent correlation in the baseline case demonstrated that a uniform stress could be used to predict crack growth in a plate with large stress gradients. Additional modeling was done to try to directly use the measured stress gradient for predictions, but no improvement in accuracy was attainable. In fact, using the low stress values at the interior of the plate predicted low initial growth rates while the stress values at the exterior of the plate predicted the higher than observed final crack growth rates. Therefore it is recommended that a uniform stress be used to represent a stress gradient across a plate or stiffened plate. The location to measure this uniform stress should be near enough to the crack line that little

increase in stress would be expected to be seen at the crack line. In other words, the stress should be taken as the stress acting on *that* cross section and not a true “remote stress” as the analytical formulations theoretically apply to.

8.3 CASE 1: SOLID STIFFENERS

Many analyses are presented in Figure 8-3 to illustrate the effect of various modelling assumptions. Curves A and B illustrate that identical predictions will be obtained through the finite element modeling technique and analytical modeling provided the same assumptions are used. Prediction A was made using a F.E. analysis without gap elements and compressive residual stress of -70 MPa between weld lines. A similar result was obtained with the analytical model by matching the F.E.A. K_r (Curve 5 of Figure 7-3) and using the net section coefficient (Finite width correction). This curve is shown as Curve B.

Curve D was obtained by repeating the analysis used in Curve B with the exclusion of the finite width correction. This exclusion models any effects of displacement-controlled

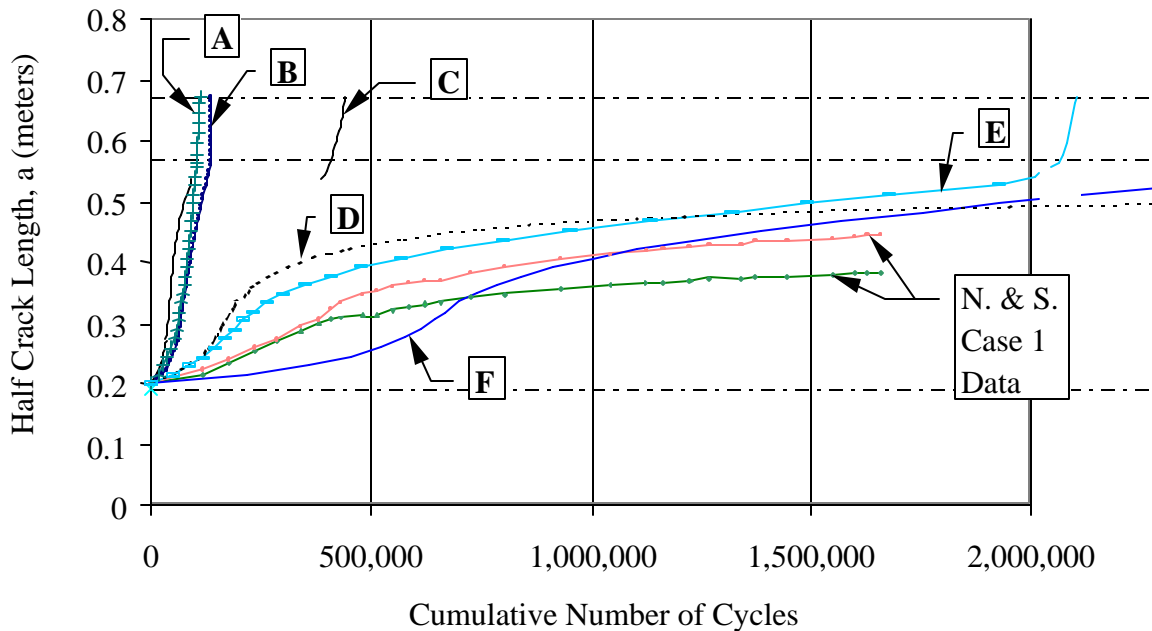


Figure 8-3: Predictions made for Case 1: Solid Stiffeners.

loading more effectively. There is significantly better accuracy obtained by removing the net section coefficient. The unconservative growth rate exhibited in curve D is attributed to the high compressive residual stresses and subsequent K_r used in the analysis.

Prediction C is the normal analytic model prediction. It uses Faulkner's method of specifying the residual stress distribution with a triangular tensile region equal to 3.5 times the plate thickness. It is felt that this result would be very accurate had the plate been uniformly stressed without the steep gradient as seen in Figure 3-8. Low stresses in the stiffeners were also reported, and these likely promoted slower crack growth than would be present in a uniformly stressed panel.

Curve E is the result of finite element analyses made *with* gap elements and the assumption that stiffeners were immediately severed. In contrast, curve F represents the same analyses with the exception that linear interpolation was used between an unbroken and broken stiffener scenario. All of the finite element analyses were performed with no variation in the specified residual stress. A significant amount of labor is required to perform the analyses under a different set of residual stress magnitudes. As an alternative, this report demonstrates that the simpler analytical model produces the same results as the F.E. model without gap elements under the same loading conditions. Modifications in residual stress magnitudes were then investigated through the analytical model, and it is certain that a finite element model would produce identical predictions when performed under the same residual stress modifications. Variances do occur when gap elements are used in the finite element model, however. For this reason, one may contrast the effect of using gap elements in curves E and A, where gap elements represent the only variation in the F.E. modeling.

Of these analyses, prediction C provides the most reasonable prediction. The authors believe it is a reasonable prediction since it provides a conservative estimate without involving complex analysis or the fine-tuning of parameters that are highly variable. It is the analytical model that incorporates a simple estimation of the residual stress and does not

include the net section correction. Had the finite element analysis without gap elements (Curve A) been performed with lesser residual stress magnitudes, the F.E. prediction would have been very similar.

The testing of this specimen ended with cracking in remote regions of the specimen. The remote cracking, in combination with the large stress gradient, support using this conservative approach to estimate crack growth in situations where a larger structure provides a more continuous force transfer into the full stiffened plate section.

The large differences among the various analyses indicates the high degree of sensitivity of the analyses to the applied and residual stresses. The recommended analysis technique would be case C. The fact that the other analyses give widely varying results, some coincidentally in better agreement with the experimental data, should not be construed as random fudging of assumptions in order to match the data.

Cases two and three produced more uniform testing results and were not affected by any remote cracks and subsequent loss in applied stresses. For these reasons, more accurate modeling was justified and the stress gradient was directly accounted for.

8.4 CASES 2 AND 3: STIFFENED PANELS WITH CUTOUTS

Cases two and three of the experimental study gave very similar results. Consequently, refinement in the modeling could be achieved with greater certainty that the behavior could be expected in real structures. A progression of different analyses will be shown to arrive at the recommended modeling technique.

The first predictions demonstrate the inadequacy of simple rule-of-thumb coefficients applied to each CCT K result. The CCT ΔK was used without a finite width correction to produce the results shown in Figure 8-4. Rolfe's reduction factor (0.6 R.F. in Figure 8-4)

for multiple stiffeners (see Equation 2-10) was applied to the same CCT ΔK and produced highly unconservative predictions.

Note that this result using Rolfe's reduction factor would be the same for Case 1, and the curve labelled 0.6 R.F. in Figure 8-4 could also be shown in Figure 8-3. It can be seen that the result would be very unconservative for Case 1 as well..

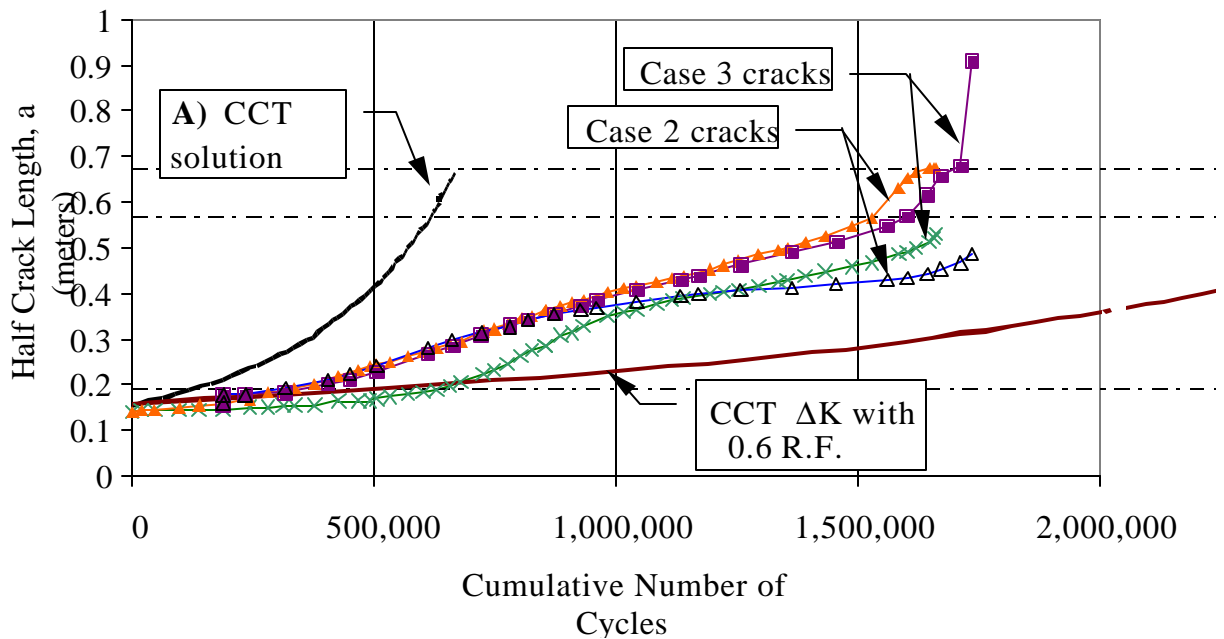


Figure 8-4: Predictions based on simple CCT ΔK without finite width correction.

The next plot, Figure 8-5, demonstrates the differences obtained in finite element modeling. By using gap elements in the finite element analysis, prediction H was made. Excluding gap elements and using simple addition of F.E. K_r and K_{app} values resulted in curve I. Both of these prediction methods showed that the specified compressive residual stress was retarding crack growth too much. Therefore, the residual stress distribution was reduced by

five percent. This reduction brought compressive stress to a constant value of -66 MPa between weld lines. The effect of the residual stress reduction is seen in curve F.

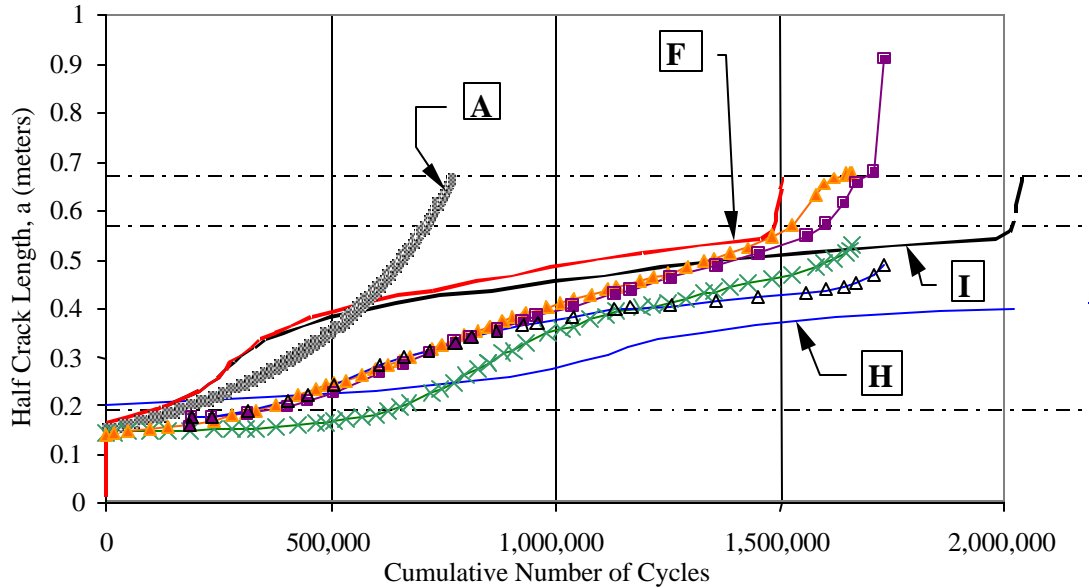


Figure 8-5: Predictions based on F.E. analyses with and without the use of gap elements.

The finite element predictions generally exhibited poor reproduction of the experimental data shape for the specified residual stress fields and applied loading. Finite element modeling is only effective if valid input is specified, such as accurate applied stresses. It was hypothesized that the poor curve appearance was attributable to both low stresses seen in the interior stiffeners and lack of restraint effects in the all the stiffeners. An investigation was conducted on this speculation to improve the prediction curve appearance. Since the analytical model could duplicate the finite element model results well, it was used as a quick means of determining a prediction that would be obtained had either model been used. Therefore, prediction refinement for cases two and three was made using the analytical model under different loading conditions. These modifications were primarily investigated in the analytical model but may be easily duplicated in finite element modeling.

The lack of stiffener restraint on crack growth was the first modification addressed. It directly addresses observations of Petershagen and Fricke, where they reported that the

stiffeners with cutouts were ineffective in slowing down an approaching crack tip. This behavior was confirmed when observing the experiments involving stiffeners with cutouts (ratholes or raised drain holes). F.E. analyses verified that there was virtually no decrease in K as a crack approached a weld access hole. The finite element method did, however, predict decreasing K -values in the case of solid stiffeners.

A better understanding of crack retardation due to geometry may be obtained by taking a closer look at the plate/stiffener interface. It is intuitive that a rathole would hinge more easily than a continuous stiffener. This is seen in Figure 8-6. However, since the crack propagates into the solid stiffener readily, the benefits of slowing down a running crack are limited.

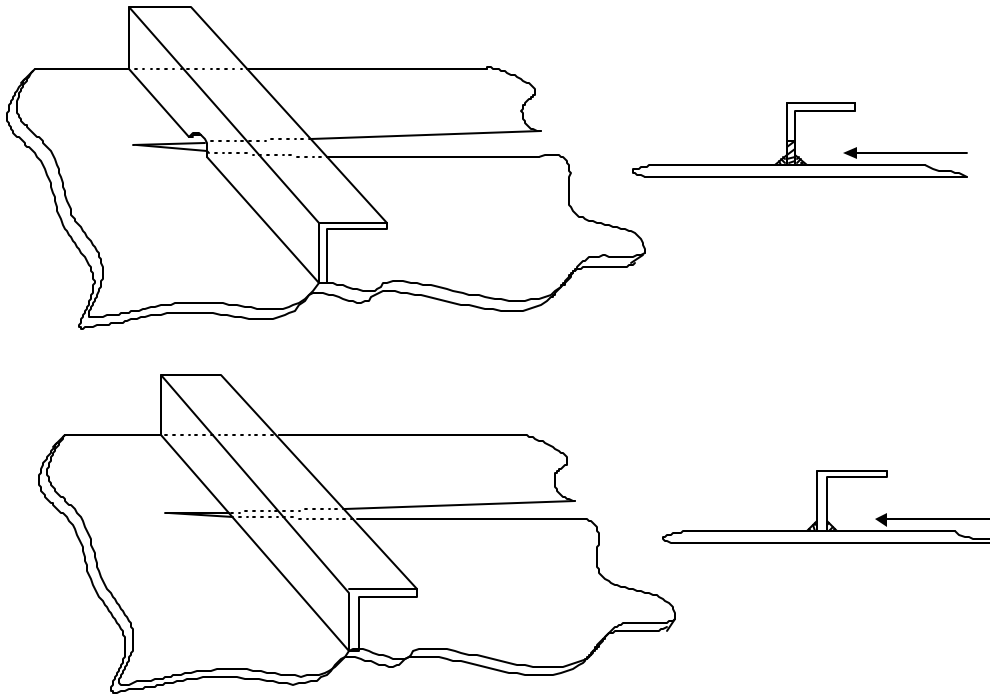


Figure 8-6: Effects of geometry on crack opening.

To accommodate the lack of stiffener restraint in panels with cutouts is relatively easy. All that is necessary in the analytical model is to set the f_1 coefficient to zero. This will

eliminate any contribution of the first effect discussed in Section 5.2 found on page 98. In the finite element model, the lack of stiffener restraint is duplicated by properly modeling the geometry of the cutout (rathole or raised drain hole).

Modeling the low stress in the stiffeners was considered next. An appropriate modification that could be made to the models was reducing the force imparted by a severed stiffener. Recall that the effect of a severed stiffener in the model is treated as a pair of splitting forces on the crack line. To reduce the magnitude of the splitting forces, the thickness of the stiffener was decreased. A smaller stiffener area translates to a smaller amount of force that the stiffener is responsible for, and the modification effectively represents a stiffener with lower stress than the plate. One can accurately model different stress levels in many stiffeners by specifying a ratio of the stiffener stress to the plate stress. In finite element modeling, decreased stress levels are automatically incorporated if the complete load path in the structure is included.

These changes were made to the analytical model and the results may be seen in Figure 8-7. Curve E was made using an exterior stiffener stress ratio of 0.68 and an interior stress ratio of 0.16. These ratios were determined from strain gage readings from atop the stiffener webs in the uncracked specimen. By lowering the interior stiffener stress ratio to 0.13 even better correlation was obtained, as seen in curve J. Both curves E and J were generated with the analytical model neglecting the f_1 coefficient and the net section correction. They illustrate that the analytical model can be very precise if the true stress distribution is known. Furthermore, shear lag effects in the stiffened panel may be accounted for by specifying only the individual stiffener stress ratios and an approximation to the uniform plate stress.

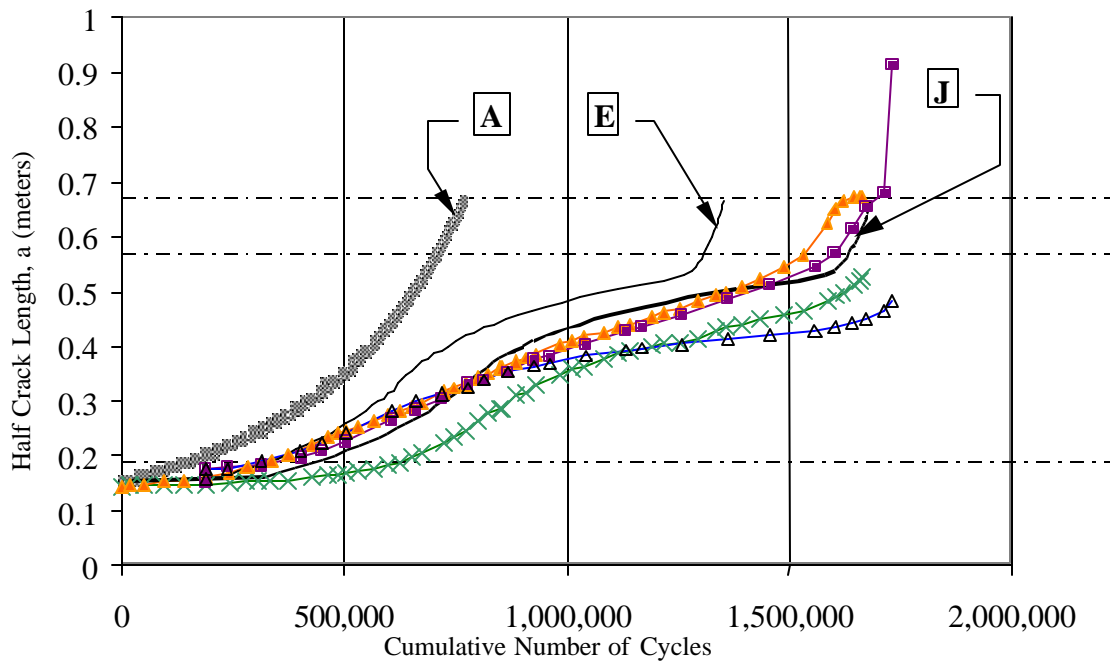


Figure 8-7: Refined analytical modeling.

The results of Figure 8-7 show much promise for the successful modeling of fatigue crack growth in stiffened panels. Curve E doubled the prediction life estimate made by curve A, the CCT ΔK prediction made assuming no stiffener or residual stress effects. The modifications to the analytical approach could easily be duplicated in finite element modeling by changing the uniform stress applied to the stiffeners into a more realistic applied stress or modeling the complete load path. The uniform stress should still be applied to the plate, however, because analyses that directly used the stress gradient underestimate crack growth rates while the crack length was less than one stiffener spacing.

For comparison, the ΔK_{eff} values for many of the predictions made for case 2 and 3 are shown in Figure 8-8. Data points in the figure represent extrapolated ΔK_{eff} values from the experimental data.

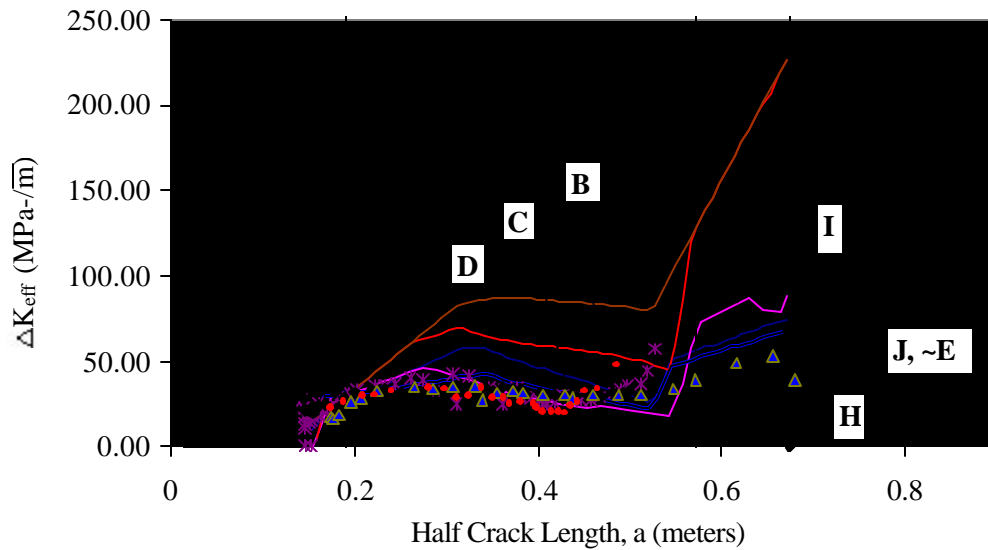


Figure 8-8: ΔK_{eff} for various prediction methods in cases 2 and 3.

Now that appropriate modeling techniques have been defined, it is important to look at some precautions that should be made in such analyses. The first and most important precaution is to use either a good estimate of the actual stress range or a slightly conservative estimate. The stress range affects the final cycle count tremendously and if one wishes to obtain an accurate or conservative measurement, due care should be exercised. Secondly, analyzing several starting crack lengths is essential—especially for situations where the initial crack length may be affected by compressive residual stresses. To illustrate, consider Figure 8-9. Curve G was made using the actual starting crack length of 316-mm, where the crack was theoretically located in a compressive residual stress zone. This theoretical value of residual stress exceeded the actual residual stress distribution and caused extremely low ΔK_{eff} values to be obtained. Consequently, the prediction made gave an extremely high number of cycles necessary to propagate the crack a short distance. On the other hand, using an initial crack length of 322-mm, in the exact same analysis, resulted in the prediction seen as curve C.

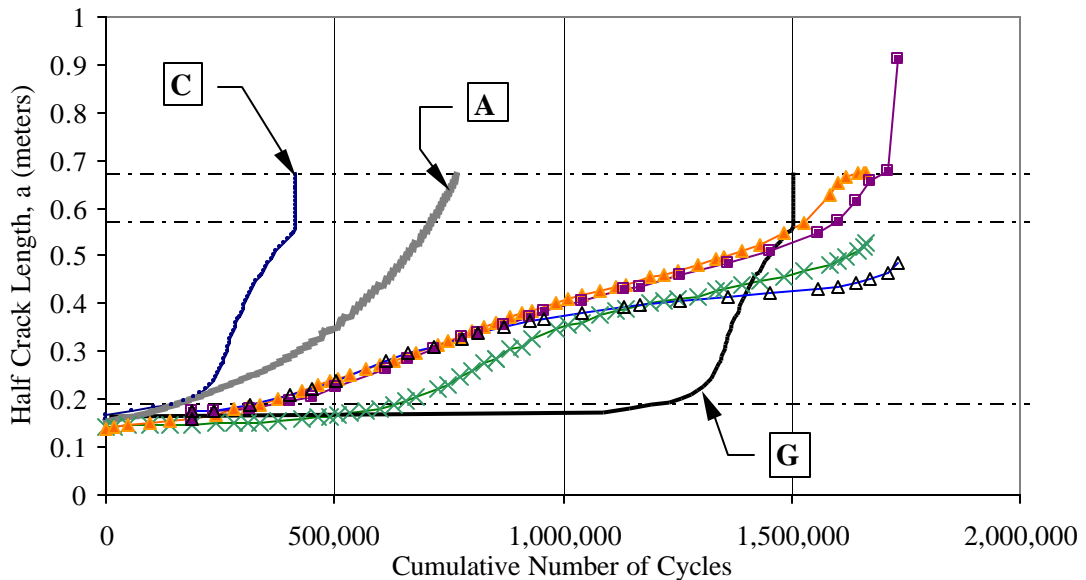


Figure 8-9: Possible prediction variation for cracks growing out of initial residual stress zone.

The wide range is not an error in modeling procedure. Rather, it illustrates that the variability in residual stress may cause limited success in small crack growth estimates. A small crack growth estimate in the course of this study means a crack less than one stiffener spacing in length. To alleviate any unconservative estimates for small cracks, one could set the compressive residual stress in the first stiffener span to zero.

8.5 CASE 4: STIFFENERS WITH RATHOLE AND MASTER BUTT WELD

Case four showed accelerated crack growth more typical of a plate specimen than a stiffened panel. Therefore, predictions were appropriately made by using variations on the simple CCT stress intensity factor without accounting for any residual stress interaction.

The resulting predictions may be seen in Figure 8-10. Curve A was made using a finite width correction factor and a stress range as determined in the same fashion as developed in

section 8.1. Instead of using the net section correction to account for specimen finite width, a simple secant formula was used:

$$f_w = \sqrt{\sec\left(\frac{pa}{2b}\right)}$$

where $2a$ is the half-crack width and $2b$ is the total plate width taken as the plate width plus the 30.5-cm edge webs.

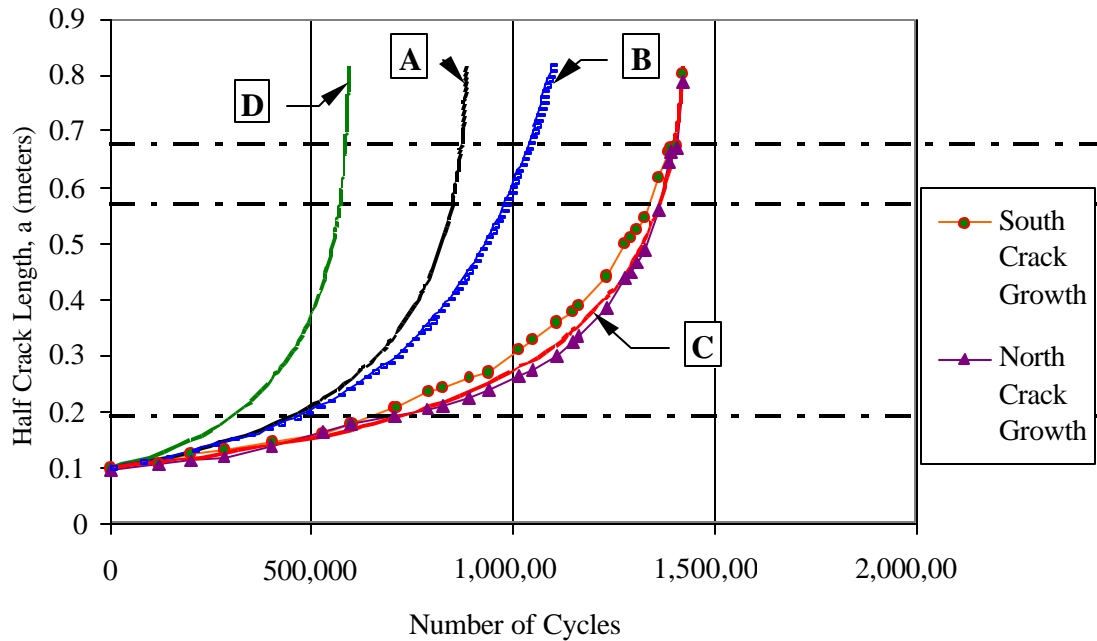


Figure 8-10: Case four predictions.

This finite width correction was used for both its simplicity and because the net section coefficient did not perform well under the current testing configuration. The net section coefficient yielded higher amplification than was probable for shorter crack lengths in the plate. The secant formula, however, exhibits a delayed amplification until the majority of the plate is cracked. This behavior better suited the observations in the experiment. It should be noted that the secant formula does not usually include the width of the edge webs, but it certainly is not appropriate for a plate with stiffened edges. Therefore, the inclusion of the

edge web plates in the total plate distance was a compromise between a theoretical application and real world observations.

Curve B represents the same analysis without the finite width correction. Finally, curve D was made using the suggested weight function of Petershagen and Fricke to account for stiffener separation:

$$f_s = \frac{2b_s t + A_s}{2b_s t} \quad \text{Eqn. 8-1}$$

where b_s is the distance between stiffeners, t is the plate thickness, and A_s is the cross sectional area of the stiffener. This coefficient was applied to the CCT K solution in the following manner:

$$K_I = f_s f_w (s_n \sqrt{pa}) \quad \text{Eqn. 8-2}$$

In making these predictions, it was quite noticeable that the actual fatigue data could be better mapped by deterring from the stress range definition determined in section 8.1.

Iterating on the stress range resulted in an excellent data fit for $\Delta\sigma = 35$ MPa. This prediction, curve C, includes the finite width correction used in prediction A. Trial and error is not an option for practice, however, and therefore a reasonable expectation should fall in the range of curves A, B and D. For case four it is recommended that the CCT K should be used in conjunction with the secant finite width correction.

8.6 CASE 2A: MULTIPLE SITE DAMAGE IN STIFFENERS WITH RATHOLES

Case 2a represented a stiffened panel with cracks initiating at weld access holes (ratholes). A complete description of the experiment was made in Section 4.6 on page 92. The objective was to simulate four cracks at adjacent stiffeners in a wider structure than the test specimen. The configuration of the test specimen forced several compromises. The stiffener proximity to the edge webs and the large stress gradient across the panel were

problems. The results of the test, therefore, are of limited use in developing a refined model that would work well in realistic applications.

A simplified and conservative analysis was promoted based on the information from the test. The prediction approach was similar to that of case four, where the CCT K was applied and modifying coefficients investigated. The resulting model is developed in two stages: Stage one is shown in Figure 8-11 and stage two in Figure 8-12.

Stage one involved making six predictions based on the CCT K equation. First, a prediction curve is made for each crack tip except those propagating away from the exterior stiffeners. A new crack length definition is used in the CCT K formula:

$$K_{mc} = s \sqrt{pc} \quad \text{Eqn. 8-3}$$

where c is the distance of the crack tip from the stiffener centerline.

This crack length was defined because sometimes the crack length would not be symmetric about a stiffener, and best results were found if this definition was used. For the crack tips propagating away from the exterior stiffeners, no K was determined directly. Rather, the incremental crack growth was defined as twice that of the crack tip on the interior side of the same stiffener. The stress values were taken from the values along each respective stiffener line. For example, for the interior stiffeners the stress was determined by estimating the stress at the stiffener line and approximately 20-cm from the crack line in the uncracked body. The results of this first phase may be seen in Figure 8-11.

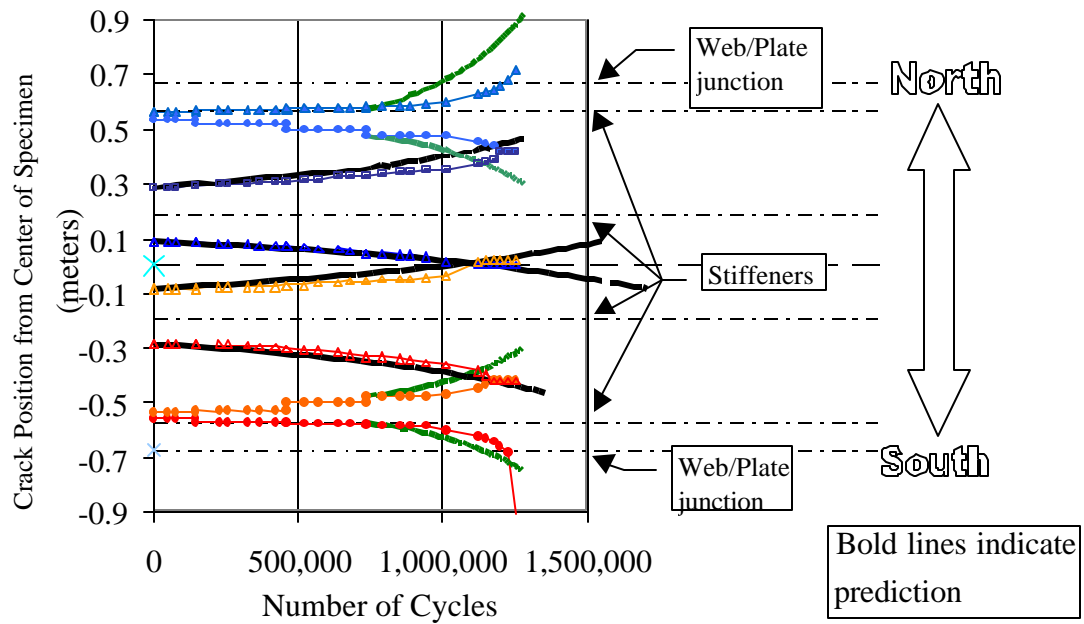


Figure 8-11: Stage one of prediction for case 2a.

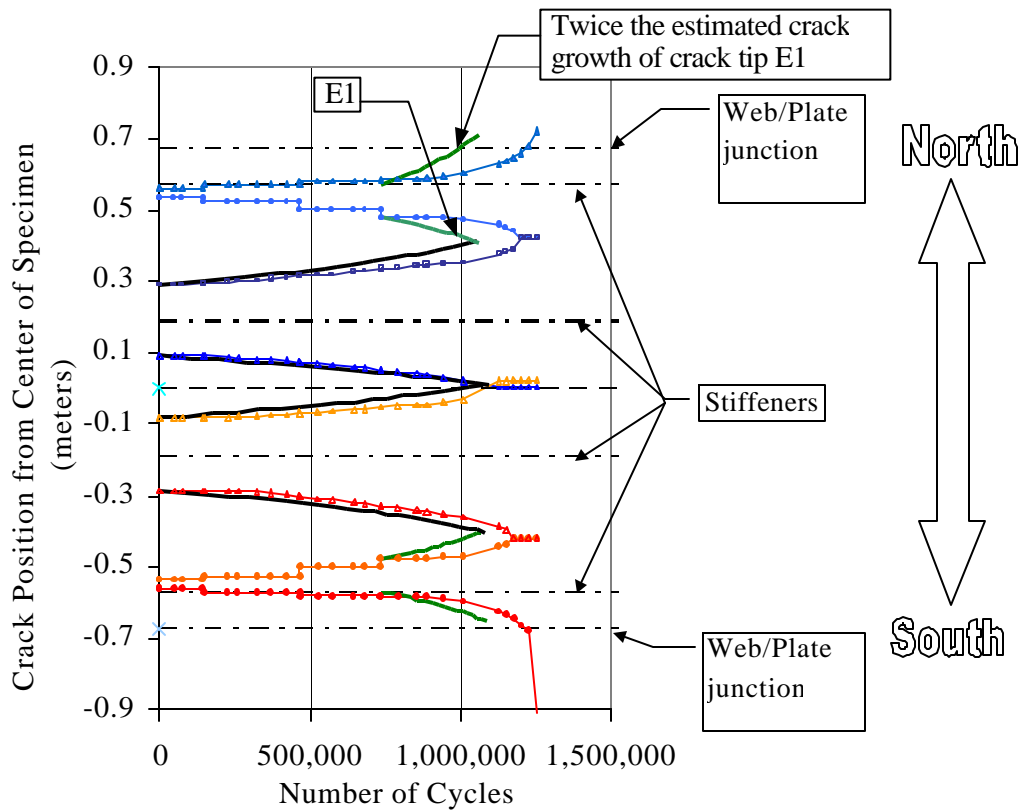


Figure 8-12: Beginning of stage two of prediction for case 2a.

The prediction of stage one generates crack lengths that overlap rather than grow together. By plotting the predictions, we may visualize number of cycles necessary for the cracks to merge. This cycle count is determined by a stage one prediction. Next, the crack is treated as a continuous crack similar to those modeled in the previous specimens. The continuous crack may be seen in Figure 8-12, where the stage one predictions have been cut off to represent merged crack tips. Any prediction made assuming the crack is continuous comprises a stage two prediction. Since the specimen width prevented continued growth of the crack, no stage two prediction was made.

The approach may be considered crude but offers a conservative model for assessment in light of the uncertainty in the test results. Estimating the extreme stiffener crack tips as twice the interior half provides a safe yet feasible behavior in the configuration. Undoubtedly better models could be created if multiple, wider specimens were involved in the experiment. However, loading and financial limitations make such a study impractical.